Solar Energy 286 (2025) 113196

Contents lists available at ScienceDirect

Solar Energy

journal homepage: www.elsevier.com/locate/solener

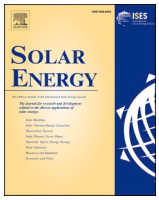

A next-generation greenhouse design for increasing solar gain in high-latitude regions

Kishin Matsumori [a], Martin Leigh [b], Ian A. Howard [a,c], Gan Huang [a], Bryce S. Richards [a,c,*]

[a] Institute of Microstructure Technology, Karlsruhe Institute of Technology, Hermann-von-Helmholtz-Platz 1, 76344 Eggenstein-Leopoldshafen, Germany
[b] Ampode Limited, 28 Foxhall Road, Timperley, Altrincham, Cheshire, WA15 6RP, United Kingdom
[c] Light Technology Institute, Karlsruhe Institute of Technology, Engesserstrasse 13, 76131 Karlsruhe, Germany

ARTICLE INFO

Keywords:
Greenhouse
Agriculture
Solar energy
Sunlight diffusion
Optical engineering
Ray-tracing simulation

ABSTRACT

Greenhouses create microclimates suitable for growing vegetables under less favourable outdoor climatic conditions. In high-latitude regions, greenhouses are used to extend the growing season in winter, when the temperature is low and daylight hours are short for vegetable growth. This work presents the optical design of a novel greenhouse that can increase the amount of sunlight available to plants. The design consists of a double-walled plastic film with tube-like pockets to form the greenhouse roof. Water flowing inside the plastic-film pockets refracts light, allowing sunlight to be captured more efficiently compared with conventional planar sheets when the solar elevation angle remains small (in winter). Ray-tracing simulations are conducted, and the solar-harvesting performance of the water-tube greenhouse design is evaluated in Cheshire, northwest England (latitude: 53.18° N). The simulation results suggest that the water-tube greenhouse is beneficial for extending the growing seasons in Cheshire. For example, the water-tube greenhouse can capture 67% more sunlight in the early morning in winter compared with a conventional polytunnel greenhouse.

1. Introduction

The number of people who cannot access sufficient quantities of healthy and nutritious foods is increasing. According to the Food and Agriculture Organization of the United Nations (UN), it was estimated that 690–783 million people experienced hunger in 2022 [1]. To address this challenge, advancements in agricultural technology are essential, especially in regions where traditional farming is hindered by extreme climates. One promising solution is the use of greenhouses, which allow for the cultivation of crops in environments where outdoor farming is not feasible. In high-latitude regions, characterised by short summers and long, cold winters, growing seasons are significantly limited. By controlling the internal climate (e.g. interior temperature, relative humidity, and carbon dioxide concentration [2]), greenhouses can extend these seasons and increase food production [3], thus contributing to global food security efforts. Technological advancements offer further enhancements for extending growing seasons in harsh climates, such as heating systems to regulate interior temperature [4–7], the integration of photovoltaics for electricity generation to supplement energy needs in greenhouses [8–10], monitoring systems to automatically control the greenhouse's microclimate [11,12], as well as the use of LED lighting to provide additional light for plant cultivation [13,14]. While such active systems play a critical role, advancements in passive approaches that do not rely on energy sources, are fundamentally important to extend growing seasons.

In high-latitude regions, a key factor for greenhouses is maximising solar gain for plant growth during the winter months, which will be addressed in this study. One of the most crucial design considerations to enhance sunlight exposure during this season is determining their optimal orientation – defined as the long axis of the greenhouse (Fig. 1**a**) [15–19]. The optimal greenhouse orientation differs depending on the chosen geographic location. For the northern hemisphere, several theoretical and experimental studies suggested that east–west (EW) orientation is beneficial compared to north–south (NS) orientation because a greenhouse with EW orientation receives less solar radiation in summer and more in winter than one with NS orientation [11,12,16–21]. This orientation allows for better management of solar gain throughout the year, minimising overheating during summer while maximising sunlight capture during winter to support plant growth.

The difference in light capture due to greenhouse orientation can be

* Corresponding author at: Institute of Microstructure Technology, Karlsruhe Institute of Technology, Hermann-von-Helmholtz-Platz 1, 76344 Eggenstein-Leopoldshafen, Germany.
E-mail address: bryce.richards@kit.edu (B.S. Richards).

https://doi.org/10.1016/j.solener.2024.113196
Received 6 August 2024; Received in revised form 10 December 2024; Accepted 12 December 2024
Available online 17 December 2024

described by considering the sun path in summer and winter (Fig. 1**a**) [20]. When the sun's elevation is high (summer), the east- and west-facing walls of an NS-oriented greenhouse receive more solar radiation than the north- and south-facing walls of an EW-oriented greenhouse, resulting in a high solar gain for NS orientation. When the sun's elevation is low (winter), the south-facing wall captures sunlight the most among all walls. The south-facing wall of the EW-oriented greenhouse is larger than the that of the NS-oriented counterpart; therefore, EW orientation is advantageous to increase solar gain in winter. These differences in solar gain become greater at higher latitudes [20]. In addition to increasing solar gain in winter, it has recently been demonstrated that EW orientation is preferable to increase the canopy light interception of tomato plants in autumn–winter-spring [22].

As discussed earlier, previous research has extensively examined the impact of greenhouse orientation on solar gain efficiency. However, these studies primarily focus on greenhouses constructed with transparent plastic covers and do not consider the potential benefits of using alternative covering materials. Up until now, various covering materials have been investigated to improve the light management of greenhouses [23–30]. For example, it is known that light-scattering films may be beneficial to enhance crop yields since incoming diffuse sunlight can be uniformly distributed on crops [31–33]. More advanced covering materials use luminescent materials to modify the colour of the incident sunlight to better match the photosynthetically active radiation (PAR) spectrum required for healthy plant growth [34–36]. While significant progress has been made with covering materials, efficient sunlight capture remains crucial, especially in high-latitude regions. Critten conducted extensive studies on the light transmission of greenhouses to enhance solar gain during winter in high-latitude regions like the United Kingdom [37,38]. To improve the sunlight-capturing efficiency of greenhouses, he suggested incorporating additional reflective materials to capture sunlight passing through the north-facing wall when the sun's elevation is low [39,40], which has also been studied by other researchers [41]. Although this method shows promise in reducing solar energy losses, it can create glare, which complicates indoor operations. Critten also investigated the light refraction properties of plastic films structured with small prisms, demonstrating that such refractive films can enhance sunlight capture in greenhouses [40]. Recent advancements in nanotechnology have enabled the large-scale production of films with complex structures [42]. However, manufacturing such films on the scale needed for greenhouses continues to be technically challenging.

Here, an innovative approach is proposed to address those issues and further advance the greenhouse technology for high-latitude regions. The proposed design involves integrating water tubes into the plastic sheeting of a polytunnel (Fig. 1**b**). The water tubes are made via a double-walled "pocketed" polymer film and heated/cooled water could flow inside the tubes. This design avoids the use of reflective films and the need for small, intricate structures like Critten's grooved films [40], potentially making large-scale production more feasible. Water has been utilised for thermal management in greenhouses [43], but the aim of the proposed system is to improve the sunlight-capturing performance of greenhouses (Fig. 1**b**). Since the water tubes can refract incoming radiation into many different angles, via acting as an optical lens, it is hypothesised that the water-tube greenhouse may be able to: i) redistribute the direct sunlight uniformly on the greenhouse floor; and ii) to capture sunlight at a low elevation angle more efficiently in winter, so that the growing seasons can be prolonged.

This study investigates the optical properties of the water-tube greenhouse and evaluating its potential to extend the growing seasons in Cheshire, in northwest England. For optical characterisation of the water-tube greenhouse performance, ray-tracing simulations were conducted for three different days in different seasons (summer solstice, autumn equinox, and winter solstice) and for three different times on each day. The simulation also considered different orientations (NS *vs.* EW) of the greenhouse. The solar irradiance and distribution on the floor of the greenhouse were measured for each parameter set (day, time, orientation). The simulation results suggested that EW orientation is beneficial to achieve high solar gain in winter in Cheshire. Compared with a conventional film-based greenhouse, the water-tube greenhouse reduces the solar gain in spring-summer-autumn. In contrast, the light distribution of the water tube enhances sunlight-capturing and distribution in winter. Especially in the early morning in winter, the water-tube greenhouse can receive 67 % more sunlight than the conventional one, indicating a potential to extend the growing seasons.

2. Methods

2.1. Simulation models: Planar-film and water-tube greenhouse

The simulation model of a conventional greenhouse (polytunnel) composed of a planar film is illustrated in Fig. 2**a**. This greenhouse is used as a reference to investigate the performance of the water-tube greenhouse, which will be introduced below. The thickness of the greenhouse's film is 0.3 mm, which is a typical thickness of a plastic film for greenhouses [23]. The refractive index of the film is 1.5, which is based on the refractive index of polyethylene [44], a commonly used covering material for greenhouses [23]. It should be noted that this

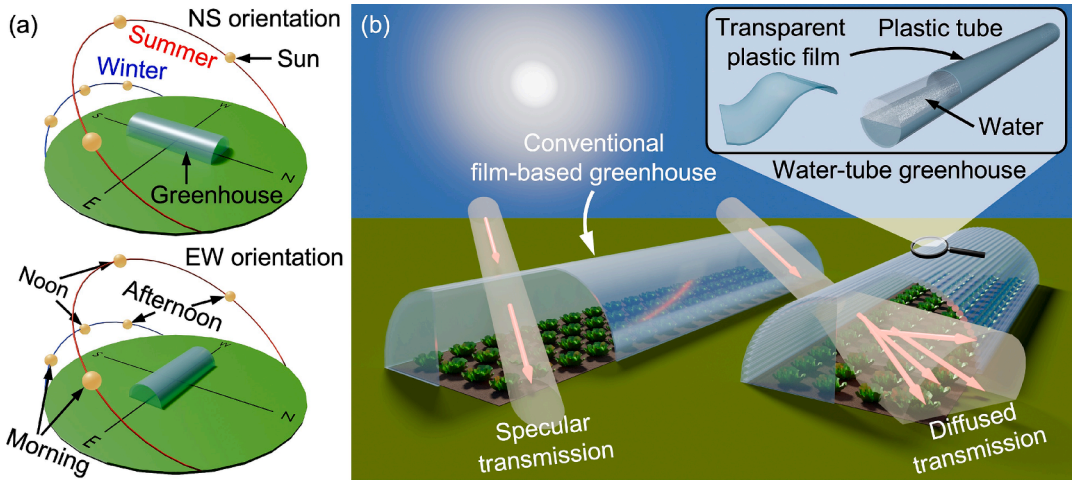

Fig. 1. (a) Schematics of NS and EW orientation of a greenhouse. The red and blue lines illustrate sun path for summer and winter. (b) Schematic of the concept of the water-tube greenhouse. In contrast to that the sunlight passes straight through the conventional greenhouse, the water-tube roof diffuses the sunlight and distributes it on the ground, increasing the solar gain.

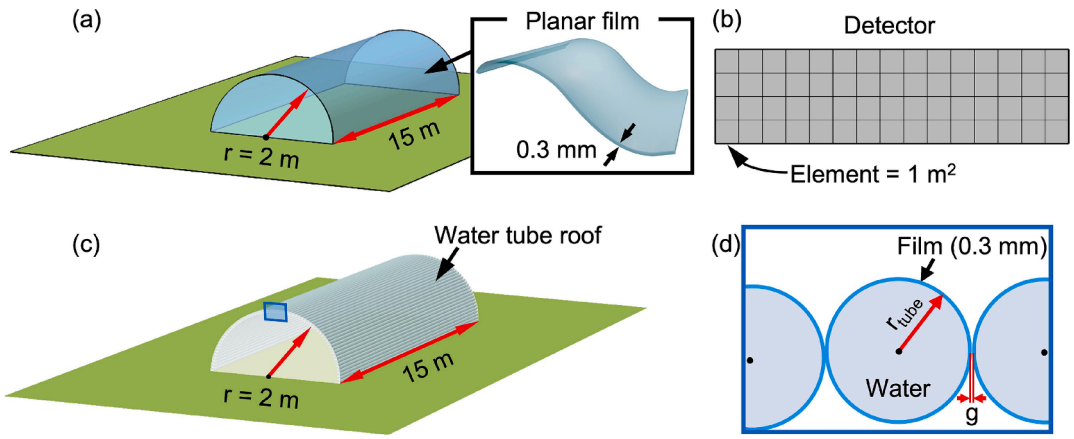

Fig. 2. Simulation models of the film and water-tube greenhouses. (a) Three-dimensional illustration of the film greenhouse which has the half-cylindrical shape (polytunnel) with a radius of 2 m and a length of 15 m. The inset shows an image of the plastic film used for the roof and the ends of the greenhouse where doors would be located. The film has a thickness of 0.3 mm. (b) Image of the detector placed on the greenhouse's floor. The detector is made of small elements (1 m^2) to measure light distribution inside the greenhouse. (c) Three-dimensional illustration of the water-tube greenhouse. Its exterior roof consists of the water tubes arranged in an arch. The arch has a radius of 2 m and a length of 15 m. The ends of the greenhouse are comprised the planar film shown in the inset of (a). (d) Enlarged side view of the water-tube arch (blue rectangle shown in c). The water tube has a cylindrical shape with a radius of r_{tube} and are filled with water. The outer surface is covered by the plastic film shown in (a). There is a very small gap between the water tubes ($g < 0.4$ mm).

investigation considers constant refractive indices (wavelength independent) for all materials for simplicity of the simulations. The greenhouse has a half-cylindrical shape with a radius of 2 m and a length of 15 m. The half-cylindrical shape was chosen for this study because it is one of the most used designs in commercial greenhouses and has been examined in past research. Its simple structure, defined primarily by radius and length, allows for easier modelling compared to other designs like the even-span type, which involves additional parameters such as roof angles. These additional parameters can affect optical performance [19], complicating general conclusions. By selecting the half-cylindrical shape, the focus remains on understanding how the introduction of water tubes influences the greenhouse's optical behaviour without the added complexity of additional structural variables.

In the simulation model, the floor of the greenhouse is covered with a detector measuring how much sunlight penetrates the greenhouse (Fig. 2**b**). The detector has small elements with a size of 1 m^2 to evaluate the light distribution properties of the greenhouse. Since the width and length of the greenhouse are 4 m and 15 m, the detector has 60 elements in total. For all simulations, no plants are placed on the detector (no shading of plants).

The simulation model of the water-tube greenhouse is presented in Fig. 2**c**. This system uses water due to its excellent optical properties in the visible range and its reusability. To maximise sunlight capture, energy losses by materials' light absorption must be minimised. Since water is transparent in the visible light spectrum, it is ideal for light dispersion. Additionally, the water used in the water-tube greenhouse can be repurposed for irrigating crops. This greenhouse has a water-tube arch as its exterior roof. There are no water tubes on the ends of the greenhouse where doors would be located. The radius of the water-tube arch (exterior roof) is 2 m and the length is 15 m. The water-tube greenhouse has the same detector on its floor. Fig. 2**d** gives the enlarged view of the water-tube arch. The radius of the water tube is given as r_{tube} (5 cm, 2.5 cm, and 1 cm are investigated in this study). There is a small gap ($g < 0.4$ mm) between the water tubes. The thickness and refractive index of the water tube's film are 0.3 mm and 1.5, respectively. The refractive index of water is 1.33 [45]. It must be mentioned that the design of the water-tube greenhouse does not include consideration for practical aspects: the mechanical strength of the water tubes, the underlying construction to hold the water-tube arch, and so on.

2.2. Location, date, and time

The light-capturing performance of the greenhouses was examined in Cheshire in northwest England (latitude: 53.18° N, longitude: 2.59° W). To select days and times for ray-tracing simulations, the sun's position in Cheshire was considered (azimuth φ and elevation θ angles in Fig. 3**a**). In general, the sun's elevation is the highest on the summer solstice (60.27° on 21st June) and the lowest on the winter solstice (13.38° on 21st December) in the northern hemisphere. On the spring and autumn equinoxes (21st March and 21st September), the sun's maximum elevation is 37.82° at solar noon. Since autumn and spring are the same elevation, it sufficed to select the following three days: 21st June, 21st September, and 21st December.

Fig. 3**b** depicts the sun's position (azimuth and elevation angles) during these three days. The numbers shown next to the marks of the plot are time, which takes summertime (daylight saving) into account. From the plot, the movement of the sun throughout the day is nearly symmetrical, meaning that the sunlight distribution in the morning is mirrored in the afternoon. In Fig. 1**a**, greenhouses with NS and EW orientation are illustrated. The symmetrical nature of these two greenhouse orientations means that by analysing the solar gain during the morning hours, it is possible to reasonably estimate the performance of the greenhouse in the afternoon without the need for extensive additional simulations. Therefore, morning was only considered for the simulations. Table 1 summarises the days and times chosen for this study. The azimuth and elevation angles of the sun on those days and times are listed in Table 2. The measuring times were selected as early morning, late morning, and noon. Only hours and minutes were used for the measuring times in this study, seconds were omitted. The time interval between them was given as 3, 2.5, and 1.5 h for June, September, and December, respectively. Noon time, where the sun's elevation becomes the highest, slightly varies for days because of an analemma [46]. The specific time points were chosen because the sun's position shifts gradually throughout the day, with both the elevation and azimuth angles changing steadily. Previous research has shown that greenhouse irradiance varies in a smooth pattern relative to the sun's movement, without abrupt changes at any particular moment [18–20]. Thus, by examining these three specific time points in the morning, the irradiance can reasonably be inferred between them, and a clearer understanding of how irradiance changes throughout the morning can be gained while also minimising computational costs.

It must be noted that the selected day and time points were

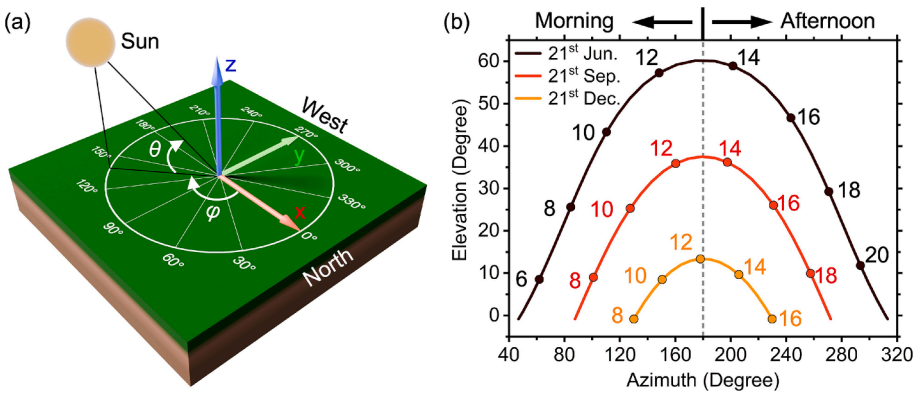

Fig. 3. (a) Schematic illustration of the sun's position. (b) Azimuth and elevation angles of the sun in Cheshire on three cloud-free days: 21st June, 21st September, and 21st December. The numbers next to the marks show the time based on the summer time, using data from [46].

Table 1
Date and time for the greenhouse simulations.

Date	Early morning	Late morning	Noon
21st Jun.	07:00	10:00	13:12
21st Sep.	08:00	10:30	13:03
21st Dec.	09:00	10:30	12:08

Table 2
Azimuth and elevation angels of the sun (data was taken from [46]).

Date	Early morning		Late morning		Noon	
	Azimuth	Elevation	Azimuth	Elevation	Azimuth	Elevation
21st Jun.	73.17°	16.82°	110.34°	43.32°	179.93°	60.26°
21st Sep.	100.91°	9.02°	134.94°	28.68°	179.83°	37.51°
21st Dec.	137.72°	3.22°	157.17°	10.47°	179.92°	13.38°

specifically chosen to assess the greenhouse's optical performance under varying solar angles throughout the year. These points do not represent typical daily conditions or peak sunlight hours, as the simulations described later neither include historical weather data nor account for diffuse sunlight effects.

2.3. Ray-tracing simulation

For the optical characterisation of the greenhouses, the ray-optics module of COMSOL Multiphysics was used. Fig. 4 gives images of the ray-tracing simulation of this work. The simulation model was composed of a light source, greenhouse, and ground plane (Fig. 4**a**). The light source was integrated with the solar simulator implemented in COMSOL, which determines the direction of sunlight. A wavelength of 600 nm was only used in this study as this is one of the main peaks in the photosynthetic action rate spectrum [47]. The number of rays emitted from the light source was 3000 m^{-2}. To reduce the computational cost, two simplifications were made: i) all incident rays were direct sunlight, thus indirect sunlight (scattering due to clouds) was not taken into account [48]; and ii) the dimension of the light source was changed (18–56 m^2) depending on the sun's position in the sky such that sunlight (incident rays) strikes only the greenhouse's exterior surface. In other words, the sunlight that does not strike the greenhouse is not simulated. Regarding clear sky conditions, based on the weather records from the Met Office, the average sunshine durations in northwest England during summer, autumn, and winter are 166, 85, and 47 h/month, respectively [49,50]. The findings presented in this study are anticipated to be applicable and relevant for these specific periods. The intensity of the light source I_{sun} was determined by the following equations [51]:

$$I_{sun} = I_{SC} \times 0.7^{AM^{0.678}} \quad (1)$$

$$AM = \frac{1}{\cos(\Theta) + 0.50572(96.07995 - \Theta)^{-1.6364}} \quad (2)$$

where $I_{SC} = 1353$ W/m^2 is the solar constant, $\Theta = 90° - \theta$ is the zenith angle, and AM is air mass [52]. In Equation (1), the factors 0.7 and 0.678 arise from the atmospheric transparency and an empirical fit to the observed data, respectively [51]. After the sunlight strikes the greenhouse, part of the sunlight is reflected, and the rest is transmitted inside the greenhouse (Fig. 4**b**). The ray-tracing simulation considered all possible light-matter interactions (reflections, transmissions, and refractions) occurring in the greenhouses. Since there is a detector in the greenhouse (Fig. 2**b**), the amount of sunlight harvested inside the two greenhouses can be measured.

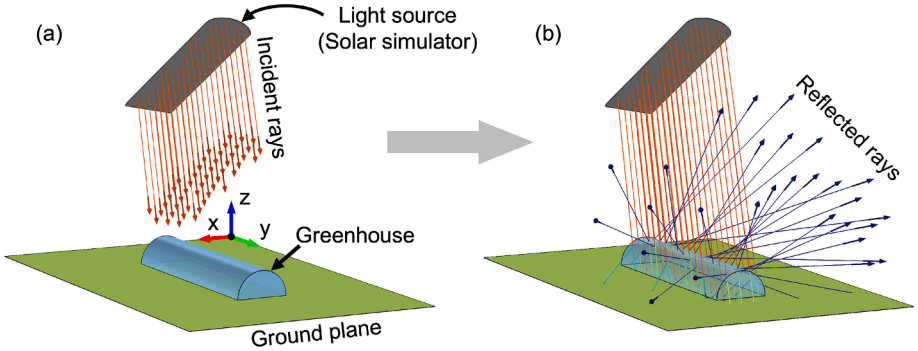

Fig. 4. Images of the ray-tracing simulation (a) before and (b) after the incident rays strike the greenhouse.

To simulate the film, the film was considered as a boundary condition; therefore, there was no physical thickness of the film in the simulation model, but the boundary condition took the effect of the thickness into account. By doing so, the computational cost can be minimised because the number of meshed elements of the simulation model can be reduced [53]. For the water tube, a cylinder was created as a domain, and the boundary condition was applied on the surface of the cylinder to consider the effect of the water tube's film. The inside of the cylinder was set as water. The computation time of the simulation per one parameter set (day, time, orientation) was up to 5 h.

2.4. Evaluation

Here, the performance evaluation of the greenhouses is described by using a worked example, which considers that the film greenhouse with EW orientation is exposed to sunlight in the late morning in autumn. An irradiance map of the greenhouse's detector is presented in Fig. 5**a**. Several figures-of-merit (FoM) were extracted from the irradiance map to quantitatively evaluate the performance of the greenhouses. The first FoM is an average irradiance (I_{ave}), which is given by averaging the irradiance of all elements over the detector. The average irradiance indicates the light transport efficiency of the sunlight into the greenhouses. The second FoM is uniformity (U), determining how uniformly the sunlight is distributed across the detector. This aspect is crucial for plant growth, as an uneven distribution of light may cause some areas to receive significantly more or less light, potentially resulting in inconsistent crop growth. Attaining a higher U value ensures a more balanced distribution of light, promoting uniform growth conditions throughout the entire cultivation area. The uniformity is defined by the number of elements having an irradiance of ± 25 % of I_{ave} ($N_{25\%}$) and the total number of elements (N_{tot}). The uniformity is given by Equation (3):

$$U = \frac{N_{25\%}}{N_{tot}} \times 100[\%] \tag{3}$$

In the modified irradiance map, which is plotted within ± 25 % of the average irradiance (Fig. 5**b**), two elements on the right top of the detector are out of the range. The remainder (58 elements) exhibit irradiance within the ± 25 % range. From these values, the uniformity of this example is given as $U = (58/60) \times 100 = 97$ %. When both the average irradiance and uniformity are high, the greenhouse is regarded as high-performance greenhouse.

To understand the average irradiance of the greenhouses more quantitatively, the correlation between the sunlight intensity and irradiance on the ground must be considered. Fig. 5**c** illustrates that sunlight strikes the ground when there is no greenhouse. Suppose that there is a planar plate with an area of A_D. This plate is placed perpendicular to the direction of the sunlight. In this situation, the plate measures a direct normal irradiance of the sunlight, meaning that the irradiance on the plate equals the sunlight intensity of I_{sun} (Equation (1)). When the sunlight is measured on the ground, the area receiving the sunlight is stretched, which is denoted as A_H in Fig. 5**c**. Using A_H and θ, a horizontal irradiance (I_H) on the ground is given by Equation (4):

$$I_H = I_{sun}\frac{A_D}{A_H} = I_{sun}\sin(\theta) \tag{4}$$

where I_H indicates the amount of solar energy that the ground receives when the sunlight does not interact with the greenhouses. This means that the greenhouse loses solar energy when $I_{ave} < I_H$. On the other hand, the greenhouses gain the energy when $I_{ave} > I_H$. The energy loss/gain q_e can be quantified by Equation (5):

$$q_e = \frac{I_{ave} - I_H}{I_H} \times 100\% \tag{5}$$

In the case of the example shown in Fig. 5**b**, the horizontal irradiance is $I_H = 397.7$ W/m^2, and the average irradiance is $I_{sun} = 381.6$ W/m^2. Thus, the loss is estimated as $q_e = -4$ %.

3. Results and discussion

3.1. North-South vs. East-West orientation

In Fig. 6, the average irradiance and uniformity of four greenhouses are shown: water-tube *vs.* planar film, and NS *vs.* EW orientation. For the water-tube greenhouse, $r_{tube} = 5$ cm is used. The horizontal irradiance given by Equation (4) is also presented with the average irradiance (the top row of Fig. 6). The irradiance maps used for Fig. 6 can be found in **Figs. S1-S4**.

For summer (Fig. 6**a-c**), the film greenhouse with NS orientation exhibits the highest average irradiance and uniformity in early and late morning. The film greenhouse with EW orientation shows superior performance at noon. Compared with the horizontal irradiance, the average irradiance of the water-tube greenhouse is always lower, meaning that solar energy is lost (Fig. 6**b**). The highest solar energy loss of the water-tube greenhouse is $q_e = -19$ % (noon) for NS orientation and $q_e = -27$ % (early morning) for EW orientation. The film greenhouse also loses solar energy, but it is less significant. The NS-oriented film greenhouse can slightly gain solar energy only in the early morning ($q_e = 2$ %). From the point of view of the water tube's light distribution, it was hypothesised that the water-tube greenhouse would distribute the sunlight more evenly than the film greenhouse. However, the uniformity of the water-tube greenhouse is lower than that of the film greenhouse for the early and late morning (Fig. 6**c**). These results may indicate that the water tube's light distribution properties work negatively in summer.

In the case of autumn (Fig. 6**d-f**), the water-tube greenhouse with NS orientation outperforms the others in the early morning. Its average

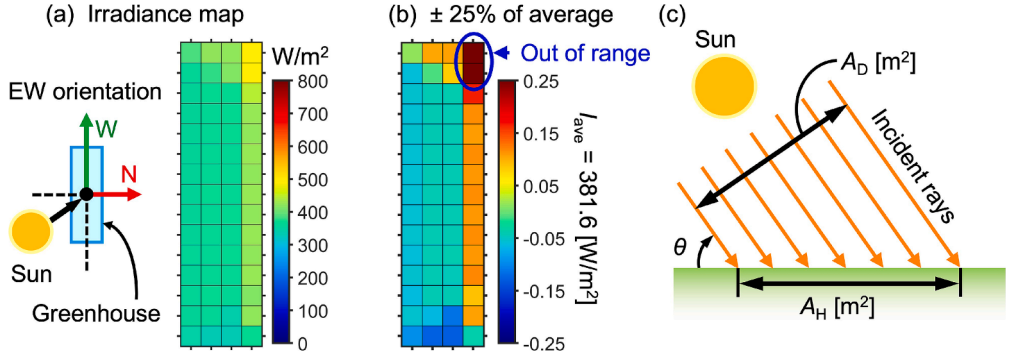

Fig. 5. Workflow of the greenhouse performance evaluation. (a) Irradiance map of the detector for the case of the EW-oriented film greenhouse at 10:30 on 21st September. (b) Irradiance map plotted within ± 25 % of the average irradiance (I_{ave} = 381.6 W/m^2). (c) Correlation between the sunlight intensity and irradiance on the ground.

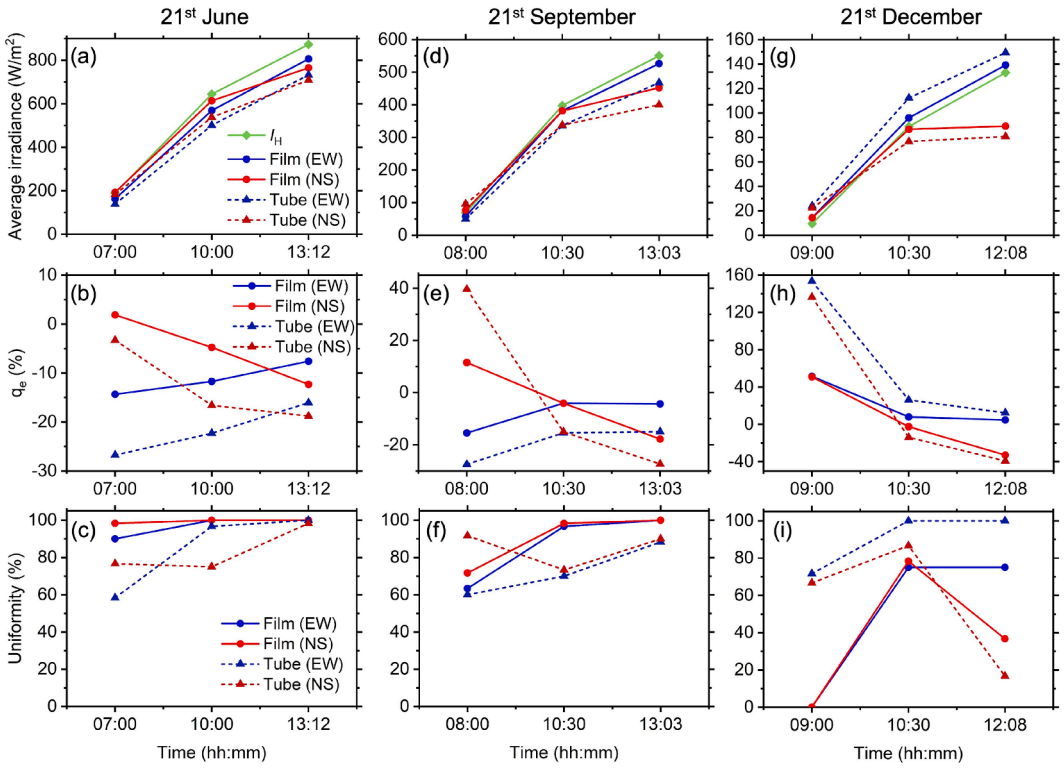

Fig. 6. Average irradiance (top row), q_e (middle row), and uniformity (bottom row) of the film and water-tube (r_{tube} = 5 cm) greenhouses for (a-c) summer, (d-f) autumn, and (g-i) winter. The red and blue circular marks with the solid line are for the film greenhouse with NS and EW orientation, respectively. The red and blue triangular marks with the dashed line are for the water-tube greenhouse with NS and EW orientation, respectively. The horizontal irradiance given by Equation (4) is also plotted in the top row (the green rhombus marks with the solid line).

irradiance is higher by q_e = 40 % than the horizontal irradiance (Fig. 6**e**). The film greenhouse with NS and EW orientation improves its performance in the late morning, and the film greenhouse with EW orientation shows the best performance at noon. The average irradiance of the EW-oriented film greenhouse shows the smallest difference to the horizontal irradiance in the late morning and noon (Fig. 6**e**). In a similar manner to the case of the summer, the water-tube greenhouse does not show positive effects on the uniformity except in the early morning (Fig. 6**f**).

Notably, the performance during winter (Fig. 6**g-i**) exhibits different trends from summer and autumn. The greenhouses with EW orientation have higher average irradiance than the NS-oriented counterparts. Surprisingly, the EW-oriented greenhouses can achieve $I_{ave} > I_H$ in the whole morning (Fig. 6**h**). The average irradiances of the film and water-tube greenhouses are higher by q_e = 52 % and q_e = 153 % than the horizontal irradiance in the early morning, respectively. These values decrease to q_e = 5 % (the film greenhouse) and q_e = 12 % (the water-tube greenhouse) at noon. The water-tube greenhouse with EW orientation shows excellent performance among all greenhouse configurations: it always has the highest average irradiance and uniformity. Its average uniformity over the whole morning is 91 %, which is high considering that other greenhouse configurations cannot achieve an average uniformity higher than 60 % (Fig. 6**i**). The uniformity of the film greenhouse is extremely low ($U \approx 0$) since all elements of the detector have values outside ± 25 % of the average irradiance, exhibiting significant variation. (**Figs. S3-S4**). Based on the established results, it can be concluded that the EW orientation is advantageous to capture more sunlight in winter, and the water tube can significantly improve light distribution inside the greenhouse.

In this study, specific crops for cultivation are not considered to facilitate a general discussion regarding the optical performance of the water-tube greenhouse. Here, the potential to grow crops during winter is explored based on the average irradiance values obtained. To assess this potential, the average irradiance needs to be converted into photosynthetic photon flux density (PPFD), which represents the number of photons of photosynthetically active radiation (PAR). PPFD levels in the greenhouses can be estimated under the assumption that their optical properties in the visible range do not significantly vary with wavelength, and that the ratio of PAR to total sunlight energy is approximately 0.48 in the UK [54,55]. The conversion from irradiance to PPFD utilises McCree's coefficient of 4.57 μmol/J for PAR [56–58]. At noon during winter, the EW-oriented water-tube greenhouse exhibits an average irradiance of 149 W/m^2, equivalent to a PPFD level of 328 μmol/m^2/s (**Fig. S5**). This PPFD level falls within the range required for growing strawberries, lettuces, and basils (250–350 μmol/m^2/s) [59–61], suggesting the potential to cultivate these crops during winter. A general summary of the PPFD level requirements for growing crops can be found in **Fig. S5**.

So far, a high average irradiance has been regarded as an indicator of a high-performance greenhouse. However, according to previous studies, the amount of sunlight entering greenhouses needs to be reduced in summer since the extensive solar gain results in an undesirable temperature increase, even for greenhouses located in northern high latitudes [11,16–18]. On the other hand, the solar gain must be maximised in winter to extend the growing seasons. The net solar gain of the greenhouse is not only determined by the average irradiance, but also by a period where the sun shines on the greenhouses. Therefore, the net solar gain increases when the greenhouses have a high average irradiance for a long period. By comparing NS and EW orientation for each greenhouse and different seasons, it can be found that the NS orientation has higher average irradiance for a longer period in summer than the EW orientation. Such a period becomes shorter in the later seasons, and the EW orientation outperforms the NS orientation in winter. These findings align with prior research, which similarly observed that the NS orientation generally receives more sunlight in summer, whereas the EW orientation proves more effective during

winter months [11]. For example, comparing the film greenhouse with NS and EW orientation, the NS orientation has a higher average irradiance than the EW orientation in the early and late morning in summer (Fig. 6**a**). In autumn, the average irradiance of the NS orientation is higher only in the early morning, and both orientations have almost the same average irradiance in the late morning (Fig. 6**d**). In winter, the EW orientation's average irradiance becomes higher than the NS orientation throughout the whole morning (Fig. 6**g**). The same can be applied to the water-tube greenhouse. Therefore, based on the previous works [11] and the findings in this work, EW orientation is found to be beneficial for both greenhouses located in northern England. Thus, only the EW-oriented greenhouses will be discussed throughout the remainder of the paper.

In addition to the film and water-tube greenhouses described above, different greenhouse designs were also investigated, such as scattering films (**Fig. S6-S10**). The comparison of different greenhouses concluded that the film greenhouse performs better than the other greenhouses for summer and autumn (**Figs. S11a-d**). In winter (**Figs. S11e-f**), the water-tube greenhouse has the best performance, where it can capture 67 % more sunlight and distribute sunlight better by 72 % compared to the film greenhouse in the early morning in winter. From these results, it was found that, from the optics point of view, the film greenhouse is advantageous in spring-summer-autumn, and the water-tube greenhouse performs best in winter. Especially, the water-tube greenhouse is advantageous to extend the growing seasons. Although the water-tube greenhouse experiences some drawbacks in summer, such as less uniform light distribution and greater solar energy loss, it may still provide enough light for crop growth. In fact, the estimated PPFD (**Fig. S5**) is more than sufficient to support crops like dwarf tomatoes (300 ~ 700 μmol/m^2/s) [62,63] and tomatoes (>640 μmol/m^2/s) [64] during the warmer months, suggesting that successful cultivation could still be achievable despite these trade-offs. It must be mentioned that these findings do not consider any other possible advantages, such as thermal management, while practical considerations (e.g. mechanical strength of the tubes and the greenhouse construction to bear the load) are not accounted for.

3.2. Optical properties of the film and water-tube greenhouses

To understand the difference in the light-capturing mechanisms of the film and water-tube greenhouses, the optical properties of the planar film and water tube are compared in Fig. 7. For the case of the planar film, the incident rays strike the planar film with an incident angle of θ_{in} (Fig. 7**a**). After the incidence of the rays, part of the rays is transmitted, and the rest is reflected. The colour of the rays exhibits their power normalised by the power of the incident rays. When the incident angle is small ($\theta_{in} = 20°$), the incident rays are mainly transmitted, and the reflection is weak. With increasing θ_{in} ($\theta_{in} = 80°$), the reflection is enhanced. For any θ_{in}, the transmitted rays pass through the film straight.

Fig. 7**b** presents the optical properties of the water tube with $r_{tube} = 5$ cm. It should be noted that the reflected rays are omitted from the picture to make a clear image (**Fig. S12**). In contrast to the planar film, the optical response of the water tube is less sensitive to the incident angle because of its circular shape. The water tube strongly transmits the incident rays, and its reflection is weak (**Fig. S12**). The water tube focuses the transmitted rays at one point, such as an optical lens, and distributes the transmitted rays in a wide angular range. The density of the transmitted rays decreases with an increase in the distance from the quasi-focal point of the water tube. In this study, the simulations are simplified by considering the wavelength-independent refractive indices of water and polyethylene film. However, it is noted that in the visible range (380–700 nm), the refractive indices of water and polyethylene vary between 1.345–1.330 and 1.514–1.489, respectively [44,45]. The influence of these refractive index variations on the light distribution within the water tube was evaluated and found to be minimal (**Fig. S13**). Therefore, it is expected the optical properties of the water-tube greenhouse to be nearly wavelength-independent in the visible range.

Having understood the optical properties of the planar film and water tube, an insight into the light-capturing properties of the greenhouses is provided by considering the greenhouses with EW orientation at noon in summer and winter. In Fig. 8, the irradiance maps of the greenhouses can be found. The ray-tracing maps (the side-views of the greenhouses) next to the irradiation maps depict how the sunlight is distributed inside the greenhouses. In the ray-tracing maps, the rays with power lower than 5 % of the incident ray's power are omitted for clarity.

First, the case of summer is considered, where the sun's elevation is the highest in the year, and the film greenhouse has the highest performance (Fig. 6**a-c**). When the sunlight strikes the film greenhouse, a large amount of sunlight passes straight the film roof, and the transmitted sunlight goes to the detector (Fig. 8**a**). This is attributed to the high average irradiance and uniformity of the film greenhouse. Part of the sunlight striking the side of the film roof is reflected because of the

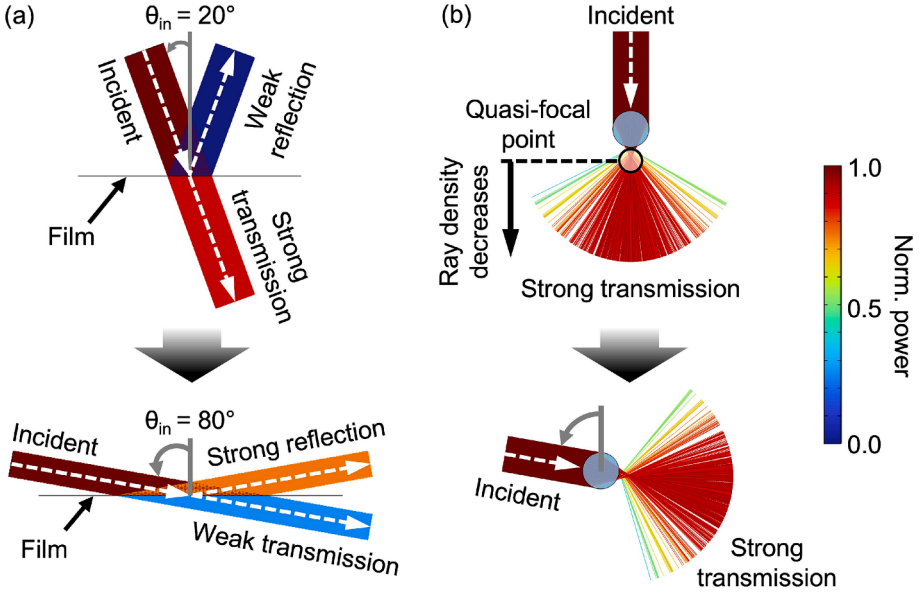

Fig. 7. Optical properties of (a) the planar film and (b) water tube. The colour bar shows the ray's power normalised by the incident ray's power.

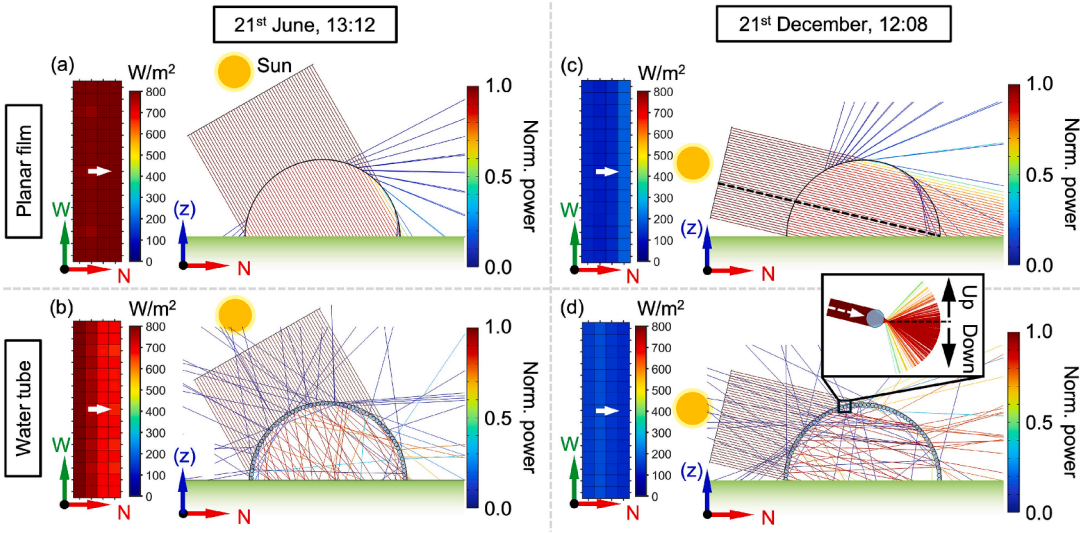

Fig. 8. Sunlight-capturing mechanisms of the film and water-tube (r_{tube} = 5 cm) greenhouses. The irradiance and ray-tracing maps are shown for the greenhouses in (a-b) summer and (c-d) winter. For all cases, EW orientation at noon is considered. The white arrows in the irradiance map present the direction of the sunlight. The ray-tracing maps do not show the rays with power lower than 5 % of the incident ray's power to make the images clearer.

high incident angle at the film surface. For the water-tube greenhouse, the sunlight is randomly distributed in the greenhouse because of the lens-like effect of the water tube (Fig. 8**b**). Some of the sunlight is redirected toward the outside of the greenhouse, which causes undesirable opportunities for the sunlight to escape from the greenhouse. Therefore, the average irradiance of the water-tube greenhouse is lower than that of the film greenhouse. On the irradiance map of the water-tube greenhouse, it can be found that the sunlight is accumulated on the south side of the detector. This is because of the lens-like effect of the water tube. When the water tube is far from the detector, the sunlight is evenly distributed; however, the irradiance is low since the ray's density decreases with an increase in the distance from the water tube (Fig. 7**b**). On the other hand, when the water tube is close to the detector, the water tube bundles the sunlight, resulting in high irradiance and low uniformity. The distance between the water tubes and detector is close on the south side; therefore, the irradiance is relatively high on the south side.

Next, the case of winter is discussed. In this situation, the performance of the film greenhouse is low, which is attributed to the fact that a large amount of sunlight does not strike the detector. In a similar manner to the case of summer, the sunlight propagates straight inside the greenhouse after it strikes the film roof (Fig. 8**c**). However, a large amount of the sunlight escapes from the greenhouse because of the low elevation of the sun. The irradiation map shows that the irradiance is high on the north side of the detector. This is because the sunlight inside the greenhouse is reflected on the north side of the film roof and redirected to the floor. In winter, the water-tube greenhouse can outperform the film greenhouse because of its light distribution properties. As described earlier, the main reason for the low performance of the film greenhouse in winter is that the sunlight propagates straight inside the greenhouse. Additionally, its low sunlight-harvesting performance is due to the fact that only a small amount of the sunlight hitting the south-facing roof is captured on the floor (indicated by the black dashed line in Fig. 8**c**). In contrast, the water-tube greenhouse can capture sunlight across the entire south-facing roof (Fig. 8**d**). More than half of the sunlight incident on the water tubes is redirected downwards due to their geometric properties, thereby increasing the irradiance on the floor (shown in the inset of Fig. 8**d**). Thus, although there is some loss due to refraction (sunlight travelling upwards) caused by the light distribution within the water tubes, the overall gain outweighs this loss. Again, it can be seen that the irradiance of the water-tube greenhouse is high on the south side of the detector, which is also attributed to the lens-like effect of the water tube.

In addition to considering the light-matter interactions occurring at the roof, those at the doors must be accounted for when the azimuth angle of the sun is not approximately 180°. For instance, Fig. 5**a-b** illustrate the scenario with $\varphi = 134.84°$ (at 10:30 on 21st September). It is observed that the irradiance is lower around the east-facing door. This phenomenon is due to the sunlight hitting the east-facing door at a steeper incident angle compared to the south-facing roof. Consequently, the door reflects the sunlight more strongly than the roof, resulting in reduced irradiance on the east side (**Fig. S14**). Based on our established understanding of the light transmission, refraction, and reflection properties of the greenhouses, the light-capturing mechanisms for the other cases can also be understood (**Figs. S1-S4**).

3.3. r_{tube} dependency

So far, the water-tube greenhouse with r_{tube} = 5 cm has only been investigated. Considering the weight of the water (≈ 118 kg per water tube with r_{tube} = 5 cm and the length of 15 m), it may be preferable to decrease the volume of the water tube. Therefore, smaller radii of 2.5 cm (≈ 29 kg per water tube) and 1 cm (≈ 5 kg per water tube) are both examined here. Fig. 9**a** compares the performance of the EW-oriented water-tube greenhouse with different r_{tube}. The results show that the average irradiance does not significantly change for those three radii for all seasons and times. In contrast, the uniformity differs for different r_{tube} except for winter. For summer, all radii have almost the same uniformity in the early and late morning, but the uniformity for r_{tube} = 1 cm becomes lower than other radii at noon. Compared with the case of summer, the uniformity differs more significantly in autumn.

To understand this difference in uniformity, the irradiance maps of the water-tube greenhouse at noon in autumn were obtained (Fig. 9**b**). From these maps, it is found that the water tube with r_{tube} = 5 cm accumulates the sunlight on the south side of the detector. The water tube with r_{tube} = 2.5 cm also accumulates the sunlight on the south side, but the accumulation is weaker compared to the larger water tube. With decreasing r_{tube} to 1 cm, the accumulation occurs not only on the south side but also on the north side, diminishing the uniformity (**Fig. S15**). The results indicate that there is an optimal r_{tube} to improve the uniformity of the water-tube greenhouse in summer and autumn, meaning that there is a trade-off between achieving a high uniformity and realising a lightweight water-tube greenhouse. However, overall optical properties of the water-tube greenhouse can be preserved for a small

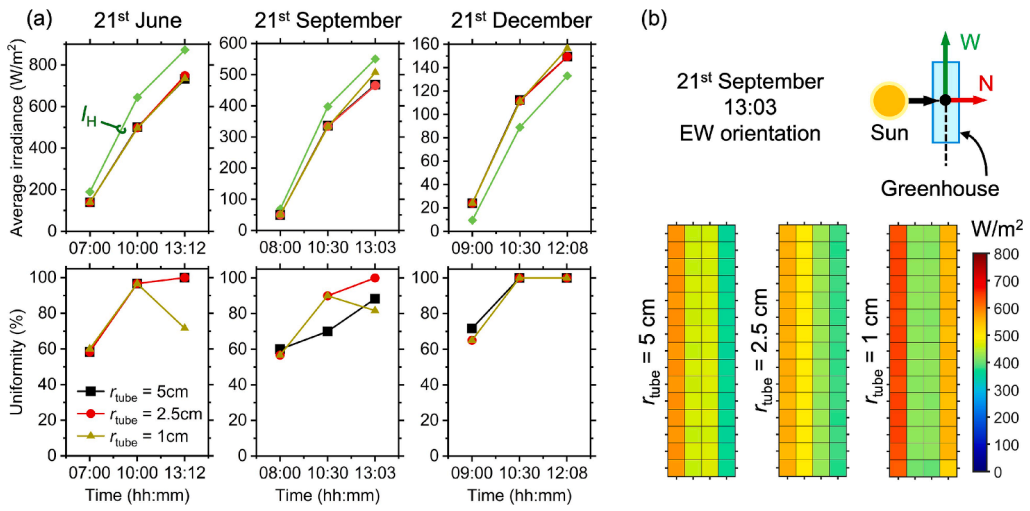

Fig. 9. r_{tube} dependency of the water-tube greenhouse. (a) The average irradiance and uniformity of the EW-oriented water-tube greenhouse with r_{tube} = 5 cm, 2.5 cm, and 1 cm. The horizontal irradiance given by Equation (4) is also plotted in the top row (the green rhombus marks with the solid line). (b) Irradiance maps of the water-tube greenhouse with r_{tube} = 5 cm, 2.5 cm, and 1 cm at noon in autumn.

r_{tube}. Since the weight of the water tube is significantly decreased by decreasing r_{tube}, it may be advantageous to design the smallest possible r_{tube} with considering the mechanical stability of the water tube and reasonable water pressure.

While consideration of mechanical stability is beyond the scope of this study, addressing its implications for the practical application of the water-tube greenhouse is essential. Materials such as reinforced transparent polyvinylchloride or high-density polyethylene could provide the necessary durability for the water tubes, as these materials can effectively support the weight of the water without requiring significant structural reinforcement. However, the total weight of the greenhouse structure will depend on the choice of tube radius, which must be factored into feasibility discussions.

For instance, based on our simulation model, using 20 tubes with r_{tube} = 5 cm results in approximately 2360 kg of water, while 40 tubes with r_{tube} = 2.5 cm equate to 1160 kg, and 100 tubes with r_{tube} = 1 cm yield around 500 kg. This considerable weight necessitates adequate support, potentially requiring stronger and more closely spaced support hoops made from materials such as galvanized steel or high-strength composites. The design of these hoops will need to be optimized to ensure the structure's integrity and safety. Since the exact design of a real-world water-tube greenhouse has not yet been defined, it is challenging to assess how tube radius impacts construction costs precisely. However, based on the simulation model, initial estimates indicate that the primary cost-saving advantage of using smaller-radius tubes comes from the reduced water weight, which could lower overall construction costs. Reducing the amount of water would also benefit the system in regions where seasonal precipitation variability or freezing temperatures could limit water availability. In Cheshire, annual precipitation tends to be stable, and winter temperatures are generally above freezing, suggesting these challenges may not be significant for the target area [50]. However, it is important to note that the feasibility of this design should be evaluated on a case-by-case basis, as climatic and water availability conditions vary by location.

Given these factors, the real-world construction of water-tube greenhouses may become feasible in future applications, enhancing their potential as a sustainable solution for optimizing solar light capture. A comprehensive approach addressing both mechanical strength and weight considerations will be vital for ensuring the practicality and efficiency of these systems.

Considering the weight of the water tube, an "air tube" (where air flows inside the tube instead of water) might initially seem more beneficial. However, light entering the air tube travels straight through, the air tube does not function as a lens like the water tube does (Fig. S16). Therefore, for enhancing the optical performance of a greenhouse, integrating water tubes into the roof structure proves advantageous.

An additional anticipated benefit of the water tubes in real applications is its potential to stabilise internal temperatures by adjusting the water temperature, allowing for cooling in summer and heating in winter. The water within the tubes, with its high heat capacity, can also serve as an effective heat buffer, passively regulating the thermal environment inside the greenhouse. This could offer significant year-round advantages for crop cultivation, though further investigation with heat transfer simulations is needed to confirm this possibility.

4. Conclusion

In conclusion, this work has investigated the optical properties of the water-tube greenhouse using ray-tracing simulations and evaluated its capability of prolonging the growing seasons of vegetables in northern England. The simulation results have suggested that an EW orientation is preferred to enhance the solar gain in winter. In spring-summer-autumn, the water-tube greenhouse possesses a lower ability to transport sunlight into the greenhouse than the conventional film greenhouse. However, in winter, the water-tube greenhouse is beneficial to capture sunlight. Especially in the early morning, the water-tube greenhouse gains solar energy efficiently: it can capture the sunlight 67 % better and distribute the sunlight 72 % more evenly on the floor of the greenhouse compared to the film greenhouse. The high performance of the water-tube greenhouse is attributed to the fact that the water tubes refract the sunlight in many different directions inside the greenhouse, which increases the chance of the sunlight striking the greenhouse's floor. This optical effect is critical to increase the solar gain at low sun elevations. In addition, the investigation of the r_{tube} dependency has indicated that decreasing r_{tube} does not significantly influence the solar-harvesting performance of the water-tube greenhouse, ensuring a lightweight system. In real applications, the shading of plants, which has not been considered in this study, must influence the solar-harvesting performance. However, considering the light distribution of the water-tube greenhouse depicted by the ray-tracing maps, it is expected its performance will not be degraded even with reasonably high plants.

Throughout this study, the focus was solely on a simple design, specifically the half-cylindrical shape. Previous research has demonstrated that optical performance varies with design [11]. Thus, exploring other designs, such as an even-span type, may further enhance

performance. Moreover, the optical performance of the greenhouses has been investigated at a specific location. Given the similarity of sun paths at the same latitude, the results obtained in this work may be applicable to regions around 53.18° N. The analysis in this work is based on specific sky conditions and selected dates to understand the optical performance of the greenhouses under different solar angles. To gain a more comprehensive understanding, future simulations should include hourly simulations covering a full year and account for both direct and diffuse sunlight using historical data. This could provide a more detailed analysis of year-round efficiency and potential improvements in design. Additionally, testing the performance in both high- and low-latitude regions would also provide insights into its broader applicability. Building upon research regarding optical performance, other practical considerations such as water management, thermal performance, and mechanical strength will need to be addressed. This will pave the way for the development of advanced greenhouse technologies capable of efficiently utilizing solar energy across diverse conditions.

CRediT authorship contribution statement

Kishin Matsumori: Writing – original draft, Visualization, Validation, Software, Methodology, Investigation, Formal analysis, Data curation. **Martin Leigh:** Writing – review & editing, Resources, Project administration, Funding acquisition, Conceptualization. **Ian A. Howard:** Writing – review & editing, Visualization, Resources, Project administration, Methodology, Funding acquisition, Formal analysis, Conceptualization. **Gan Huang:** Writing – review & editing, Visualization, Supervision, Software, Methodology, Investigation, Formal analysis. **Bryce S. Richards:** Writing – review & editing, Visualization, Supervision, Resources, Project administration, Methodology, Investigation, Funding acquisition, Formal analysis, Conceptualization.

Declaration of Competing Interest

The authors declare that they have no known competing financial interests or personal relationships that could have appeared to influence the work reported in this paper.

Acknowledgements

This work was primarily funded by PhotonHub project P2022-24 between Ampode and KIT. Further funding for KIT researchers was provided by the KIT YIG-Prep-Pro project, and Research Field Energy: Program Materials and Technologies for the Energy Transition (Topic 1 Photovoltaics and Wind Energy, ref. 38.01.05).

Appendix A. Supplementary data

Supplementary data to this article can be found online at https://doi.org/10.1016/j.solener.2024.113196.

References

[1] FAO, IFAD, UNICEF, WFP, WHO. The State of Food Security and Nutrition in the World 2023. Urbanization, agrifood systems transformation and healthy diets across the rural–urban continuum. Rome: FAO, 2023.
[2] A. Badji, A. Benseddik, H. Bensaha, A. Boukhelifa, I. Hasrane, Design, technology, and management of greenhouse: a review, J. Clean. Prod. 373 (2022).
[3] Y. Li, J. Yan, Z. Li, M. He, X. Liu, T. Li, A globalized methodology of energy-saving solar greenhouse design in high latitudes, Energy 304 (2024).
[4] I. Attar, N. Naili, N. Khalifa, M. Hazami, A. Farhat, Parametric and numerical study of a solar system for heating a greenhouse equipped with a buried exchanger, Energ. Conver. Manage. 70 (2013) 163–173.
[5] M. Kıyan, E. Bingöl, M. Melikoğlu, A. Albostan, Modelling and simulation of a hybrid solar heating system for greenhouse applications using Matlab/Simulink, Energ. Conver. Manage. 72 (2013) 147–155.
[6] Z. Xu, J. Lu, S. Xing, Thermal performance of greenhouse heating with loop heat pipe solar collector and ground source heat pump, Results Eng. 15 (2022).
[7] T. Yu, D. Wang, X. Zhao, J. Liu, M.K. Kim, Experimental and numerical study of an active solar heating system with soil heat storage for greenhouses in cold climate zones, Buildings 12 (2022).
[8] A. Boccalatte, M. Fossa, R. Sacile, Modeling, design and construction of a zero-energy PV greenhouse for applications in mediterranean climates, Therm. Sci. Eng. Prog. 25 (2021).
[9] Á. Moreno, D. Chemisana, C. Lamnatou, S. Maestro, Energy and photosynthetic performance investigation of a semitransparent photovoltaic rooftop greenhouse for building integration, Renew Energ. 215 (2023).
[10] Z. Chang, X. Liu, Z. Guo, J. Hou, Y. Su, A novel integration of supplementary photovoltaic module into compound parabolic concentrator for accelerated defrosting of solar collecting system, Renew Energ. 225 (2024).
[11] Y. Achour, A. Ouammi, D. Zejli, Technological progresses in modern sustainable greenhouses cultivation as the path towards precision agriculture, Renew Sust Energ Rev. 147 (2021).
[12] S. Ghani, F. Bakochristou, E.M.A.A. ElBialy, S.M.A. Gamaledin, M.M. Rashwan, A. M. Abdelhalim, S.M. Ismail, Design challenges of agricultural greenhouses in hot and arid environments – a review, Eng. Agric. Environ. Food 12 (2019) 48–70.
[13] S. Read, M.A. Else, P. Hadley, C. Twitchen, Reducing chill through night-break lighting and gibberellic acid application to achieve year-round UK strawberry production, Acta Hortic. 1–8 (2023).
[14] G.A. Rampinelli, R. Marcelino, J. Possenti Damasceno, C. Caroline Stalter, A.T. R. Bouchardet, G. Mohr, V. Guber, Development of artificial lighting system for light supplementation in smart greenhouses with agrivoltaic systems, Renew Energ. 231 (2024).
[15] U. Çakır, E. Şahin, Using solar greenhouses in cold climates and evaluating optimum type according to sizing, position and location: a case study, Comput. Electron. Agric. 117 (2015) 245–257.
[16] W.M. El-Maghlany, M.A. Teamah, H. Tanaka, Optimum design and orientation of the greenhouses for maximum capture of solar energy in North Tropical Region, Energ. Conver. Manage. 105 (2015) 1096–1104.
[17] M.S. Ahamed, H. Guo, K. Tanino, Energy-efficient design of greenhouse for Canadian Prairies using a heating simulation model, Int. J. Energy Res. 42 (2018) 2263–2272.
[18] C. Stanciu, D. Stanciu, A. Dobrovicescu, Effect of greenhouse orientation with respect to E-W Axis on its required heating and cooling loads, Energy Procedia 85 (2016) 498–504.
[19] B.M. Karambasti, M. Naghashzadegan, M. Ghodrat, G. Ghorbani, R.B.V. B. Simorangkir, A. Lalbakhsh, Optimal solar greenhouses design using multiobjective genetic algorithm, IEEE Access 10 (2022) 73728–73742.
[20] V.P. Sethi, On the selection of shape and orientation of a greenhouse: thermal modeling and experimental validation, Sol Energy. 83 (2009) 21–38.
[21] H. Ghasemi Mobtaker, Y. Ajabshirchi, S.F. Ranjbar, M. Matloobi, Solar energy conservation in greenhouse: thermal analysis and experimental validation, Renew Energ. 96 (2016) 509–519.
[22] Y. Li, M. Henke, D. Zhang, C. Wang, M. Wei, Optimized tomato production in chinese solar greenhouses: the impact of an east–west orientation and wide row spacing, Agronomy 14 (2024).
[23] G. Scarascia-Mugnozza, C. Sica, G. Russo, Plastic materials in european agriculture: actual use and perspectives, J Agri Eng. 42 (2011) 15–28.
[24] I. Al-Helal, A. Alsadon, M. Shady, A. Ibrahim, A. Abdel-Ghany, Diffusion characteristics of solar beams radiation transmitting through greenhouse covers in arid climates, Energies 13 (2020).
[25] G.H. Timmermans, S. Hemming, E. Baeza, E.A.J. van Thoor, A.P.H.J. Schenning, M.G. Debije, Advanced optical materials for sunlight control in greenhouses, Adv. Opt. Mater. 8 (2020).
[26] M. Vuoriluoto, A. Hokkanen, T. Mäkelä, A. Harlin, H. Orelma, Optical properties of an organic-inorganic hybrid film made of regenerated cellulose doped with light-scattering TiO_2 particles, Opt. Mater. 123 (2022).
[27] K. Mishra, C. Stanghellini, S. Hemming, Technology and materials for passive manipulation of the solar spectrum in greenhouses, Adv. Sustain Syst. 7 (2023).
[28] A. Pakari, S. Ghani, Evaluation of a novel greenhouse design for reduced cooling loads during the hot season in subtropical regions, Sol. Energy. 181 (2019) 234–242.
[29] J. Shin, I. Hwang, D. Kim, T. Moon, J. Kim, W.H. Kang, J.E. Son, Evaluation of the light profile and carbon assimilation of tomato plants in greenhouses with respect to film diffuseness and regional solar radiation using ray-tracing simulation, Agric. For. Meteorol. 296 (2021).
[30] M.M. Mogharreb, M.H. Abbaspour-Fard, Experimental study on the effect of a novel water injected polycarbonate shading on light transmittance and greenhouse interior conditions, Energy Sustain. Dev. 52 (2019) 26–32.
[31] T. Li, E. Heuvelink, F. van Noort, J. Kromdijk, L.F.M. Marcelis, Responses of two Anthurium cultivars to high daily integrals of diffuse light, Sci. Hortic. 179 (2014) 306–313.
[32] T. Li, Q. Yang, Advantages of diffuse light for horticultural production and perspectives for further research, Front Plant Sci. 6 (2015) 704.
[33] M.-T. MdlÁ, F.D. Molina-Aiz, A. Peña-Fernández, A. López-Martínez, D.L. Valera-Martínez, The effect of diffuse film covers on microclimate and growth and production of tomato (Solanum lycopersicum L.) in a mediterranean greenhouse, Agronomy 11 (2021).
[34] M.E. Loik, S.A. Carter, G. Alers, C.E. Wade, D. Shugar, C. Corrado, D. Jokerst, C. Kitayama, Wavelength-selective solar photovoltaic systems: powering greenhouses for plant growth at the food-energy-water nexus, Earth's Future 5 (2017) 1044–1053.
[35] D. Hebert, J. Boonekamp, C.H. Parrish 2nd, K. Ramasamy, N.S. Makarov, C. Castaneda, L. Schuddebeurs, H. McDaniel, M.R. Bergren, Luminescent quantum

dot films improve light use efficiency and crop quality in greenhouse horticulture, Front Chem. 10 (2022) 988227.
[36] S.M. El-Bashir, F.F. Al-Harbi, H. Elburaih, F. Al-Faifi, I.S. Yahia, Red photoluminescent PMMA nanohybrid films for modifying the spectral distribution of solar radiation inside greenhouses, Renew Energ. 85 (2016) 928–938.
[37] D.L. Critten, The effect of geometric configuration on the light transmission of greenhouses, J. Agric. Eng. Res. 29 (1984) 199–206.
[38] D.L. Critten, A general analysis of light transmission in greenhouses, J. Agric. Eng. Res. 33 (1986) 289–302.
[39] D.L. Critten, The use of reflectors in venetian blinds to enhance irradiance in greenhouses, Sol Energy. 34 (1985) 83–92.
[40] D.L. Critten, Light enhancement in greenhouses using prismatic refractors in a Venetian blind assembly, Sol Energy. 37 (1986) 313–317.
[41] M.D. Pucar, Enhancement of ground radiation in greenhouses by reflection of direct sunlight, Renew Energ. 26 (2002) 561–586.
[42] Y. Zhang, W.J. Feng, W. Zhu, X. Shan, W.K. Lin, L.J. Guo, T. Li, Universal color retrofit to polymer-based radiative cooling materials, ACS Appl Mater Interfaces. 15 (2023) 21008–21015.
[43] D. Shapiro, T. Deko, I. Itshak, D. Silverman, M. Sacks, U. Adler, I. Esquira, Y. Stigliz, An innovative way for heating greenhouses using solar energy during the winter for summer crop production, Acta Hortic. 37–44 (2014).
[44] Painter LR, Arakawa ET, Williams MW, Ashley JC. Optical Properties of polyethylene: measurement and applications. Radiat. Res. 1980,83.
[45] M. Daimon, A. Masumura, Measurement of the refractive index of distilled water from the near-infrared region to the ultraviolet region, Appl Opt. 46 (2007) 3811–3820.
[46] Sun position. https://www.sunearthtools.com/dp/tools/pos_sun.php?lang=en.
[47] S.E. Balegh, O. Biddulph, The photosynthetic action spectrum of the bean plant, Plant Physiol. 46 (1970) 1–5.
[48] NREL. Bird Clear Sky Model. https://www.nrel.gov/grid/solar-resource/clear-sky.html.
[49] E. Good, Estimating daily sunshine duration over the UK from geostationary satellite data, Weather 65 (2010) 324–328.
[50] Climate research: UK climate maps and data. https://www.metoffice.gov.uk/research/climate/maps-and-data/uk-and-regional-series.
[51] A.B. Meinel, M.P. Meinel, Applied Solar Energy: An Introduction, Addison Wesley Publishing Co., 1976.
[52] F. Kasten, A.T. Young, Revised optical air mass tables and approximation formula, Appl Opt. 28 (1989) 4735–4738.
[53] K. Sankaran, Are you using the right tools in computational electromagnetics? Eng. Rep. 1 (2019).
[54] M. Tsubo, S. Walker, Relationships between photosynthetically active radiation and clearness index at Bloemfontein, South Africa, Theoret. Appl. Climatol. 80 (2004) 17–25.
[55] P. Pankaew, E.J. Milton, J. Dash, Estimating hourly variation in photosynthetically active radiation across the UK using MSG SEVIRI data, IOP Conf. Ser.: Earth Environ. Sci 17 (2014).
[56] K.J. McCree, Test of current definitions of photosynthetically active radiation against leaf photosynthesis data, Agric. Meteorol. 10 (1972) 443–453.
[57] Z. Sun, H. Liang, J. Liu, G. Shi, Estimation of photosynthetically active radiation using solar radiation in the UV–visible spectral band, Sol Energy. 153 (2017) 611–622.
[58] A. García-Rodríguez, S. García-Rodríguez, M. Díez-Mediavilla, C. Alonso-Tristán, Photosynthetic active radiation, solar irradiance and the CIE standard sky classification, Appl Sci. 10 (2020).
[59] J. Zheng, F. Ji, D. He, G. Niu, Effect of light intensity on rooting and growth of hydroponic strawberry runner plants in a LED plant factory, Agronomy 9 (2019).
[60] Z. Yi, J. Cui, Y. Fu, J. Yu, H. Liu, Optimization of light intensity and nitrogen concentration in solutions regulating yield, vitamin C, and nitrate content of lettuce, J. Hortic Sci. Biotech. 96 (2020) 62–72.
[61] R. Sutulienė, K. Laužikė, T. Pukas, G. Samuolienė, Effect of light intensity on the growth and antioxidant activity of sweet basil and lettuce, Plants 11 (2022).
[62] X. Ke, H. Yoshida, S. Hikosaka, E. Goto, Photosynthetic photon flux density affects fruit biomass radiation-use efficiency of dwarf tomatoes under LED light at the reproductive growth stage, Front. Plant Sci. 14 (2023).
[63] Q. Liu, X. Ke, E. Goto, High photosynthetic photon flux density differentially improves edible biomass space use efficacy in edamame and dwarf tomato, Plants (basel) 13 (2024).
[64] H.P. Kläring, A. Krumbein, The effect of constraining the intensity of solar radiation on the photosynthesis, growth, yield and product quality of tomato, J. Agron. Crop Sci. 199 (2013) 351–359.